

Acoustic journal bearing – performance under various load and speed conditions

T. A. Stolarski¹⁾, R. Gawarkiewicz, K. Tesch
Gdansk University of Technology, Gdansk, Poland
¹⁾ also Brunel University London, United Kingdom

1. Introduction

Traditional non-contact bearings, such as air bearings (aerostatic and aerodynamic) and magnetic bearings are commonly used in a number of practical specialist applications.

However, magnetic bearings are unacceptable where a strong magnetic flux is harmful to the surrounding environment while a continuous supply of a large volume of clean air, never sufficiently clean for food and medical applications, from external auxiliary devices is required for air bearings (for example batteries of drilling spindles used in mass scale manufacturing), which increases the cost of their use. Also, aerodynamic air bearings are known to become unstable when lightly loaded and operating at high speeds. Therefore, alternative and radically new concepts, such as acoustic bearings, offer an exciting solution.

Acoustic levitation, being at the heart of an acoustic bearing concept, uses an acoustic wave to exert a force on objects immersed in the wave field. These forces are normally weak but can become quite large when using high frequency and high intensity waves, large enough to suspend substances against gravity force. Ultrasonic levitation (frequencies higher than 20 kHz) has been used initially for levitating small objects using a standing wave field between a sound radiator and a reflector. In standing wave acoustic levitation, the size of the levitated object is limited to less than a wavelength. Standing wave type ultrasonic levitators have been

1 designed for applications in various scientific disciplines such as material processing and space
2 engineering [1].
3

4
5 Kundt's in his tube experiment [2] in 1866, in which small dust particles moved towards the
6 pressure nodes of a standing wave created in a horizontal tube, was the first to observe
7
8 standing wave levitation. The first detailed theoretical description of standing wave levitation
9
10 was given by King [3] in 1934, which was extended by Hasegawa [4] to include the effects of
11
12 compressibility. Embleton [5] adopted King's approach to fit to the case of a rigid sphere in a
13
14 progressive spherical or cylindrical wave field. Westervelt [6,7,8] derived a general expression
15
16 for the force owing to radiation pressure acting on an object of arbitrary shape and normal
17
18 boundary impedance to show that a boundary layer with a high internal loss can lead to
19
20 forces that are several orders of magnitude greater than those predicted by the classical
21
22 theory.
23
24
25
26
27
28
29
30

31
32 Another type of levitation is the squeeze-film (or near field acoustic) levitation in which an
33
34 object (not limited by wavelength) is brought very close to a radiation surface vibrating at
35
36 high frequency. The gap is smaller than the wavelength of the generated sound, which means
37
38 that the standing wave is replaced by a gas film with pressure that varies according to the
39
40 motion of the radiation surface. Squeeze film levitation can carry higher loads than standing
41
42 wave levitation and has been widely investigated for building non-contact linear and
43
44 rotational bearings [9-13]. A contribution to the analysis of squeeze film gas non-contact
45
46 suspensions was made by one of the authors of this paper [14-19].
47
48
49
50
51
52
53

54 Earlier research fully described in [18], laid out foundation for the current acoustic bearing
55
56 concept. The early device operated in an audible range of frequencies (a few kHz) generated
57
58 by the piezoelectric transducers attached to at the bearing structure and for that reason was
59
60
61
62
63
64
65

1 unacceptable and in the need of improvement, therefor an acoustic journal bearing system
2 utilizing acoustic levitation phenomenon was proposed [20, 21, 22]. The bearing shell was
3 specially configured to secure its flexibility through the use of "elastic hinges". It could be
4 elastically deformed with desired frequency by three piezo-electric actuators (PZT).
5
6
7
8
9

10 In principle, acoustic bearing should have most of the advantages of aerostatic bearings but
11 external pressurized air supply is not needed and the bearing interface can be as simple as
12 two plain surfaces; although design consideration is needed to create high frequency
13 vibration of the bearing surfaces. From experiments [23] it is evident that acoustic pressure
14 was sufficient to support a bearing spindle system even at its stationary state during the start
15 and stop operation under a load. This system was tested experimentally for various geometry
16 configurations of the bearing shell to determine its static load supporting capacity [23]. It was
17 found that the static load capacity of the bearing depends, to a large extent, on the geometry
18 of the bearing shell. Studies, which results are presented in this paper, mainly aimed at
19 finding out how effective is the squeeze-film acoustic levitation in mitigating shaft's motion
20 within the bearing of a given geometry and operating with specified rotation speed and load.
21
22
23
24
25
26
27
28
29
30
31
32
33
34
35
36
37
38
39
40
41
42
43

44 2. Apparatus, tested bearings, and procedure

45 The search for the most effective geometry of the acoustic journal bearing and its outcomes
46 are presented elsewhere [23]. As a result of that three configurations of the acoustic journal
47 bearing were identified and selected for further experimental testing to determine they
48 performance under various load and speed conditions. Nominal bore diameter of 30 mm was
49 used all bearings tested experimentally. They had length of 50 mm. Two of the bearings were
50 made of aluminium and required the use of three foil type PZTs (piezo-electric actuators)
51
52
53
54
55
56
57
58
59
60
61
62
63
64
65

1 arranged around their circumferences. The foil-type PZTs were of rectangular shape (12 x 10
2 mm) and had thickness of 0.5 mm. They were attached to the bearing outer wall at specially
3 machined flats, spaced 120°. The third bearing was made of alloy steel and six rod-type PZTs
4 were employed. The rod-type PZT had a square cross-section (5 x 5 mm) and the length of 18
5 mm.
6
7
8
9
10

11
12
13 Since there is a complete separation of interacting surfaces by an air film therefore it was
14 thought that any special microscopic examination of their state and conditions was not
15 critically important. However, both shaft and the bearings were machined in accordance with
16 strict precision and tolerances. Surface roughness Ra was equal to or less than 0.32 µm.
17
18 Dimensional tolerances of the bearing bore and the shaft were imposed in such a way as to
19 secure effective radial clearance of 20 µm. Routine check of roundness confirmed that both
20 the shaft and the bearing bore were within prescribed limits.
21
22
23
24
25
26
27
28
29
30

31
32 The details of the three bearings used are elaborated on below where all three geometries
33 are presented and discussed.
34
35
36
37
38
39
40
41

42 2.1 Geometry of tested bearing

43
44

45 Figure 1 shows the geometry and main dimensions of the first bearing (called G1). This
46 particular geometry was arrived at on the basis of studies presented in [23]. The radial
47 clearance used was 20 µm. Aluminium was used as the bearing's material because it has low
48 coefficient of energy absorption.
49
50
51
52
53
54
55

56 Figure 2 depicts the geometry together with main dimensions of the second bearing (denoted
57 G2). This bearing has a slightly different geometry, comparing to the previous one, which was
58
59
60
61
62
63
64
65

1 arrived at through finite element modelling with the aim to obtain deformation of the bearing
2 bore (nominally a circle) closely resembling well known three lobe configuration. This bearing
3 was made of aluminium for the reason stated above. The radial clearance was 20 μm –
4 exactly the same as for the first bearing.
5
6
7
8
9

10 The geometry of the third bearing, shown in Figure 3 and called G3, is radically different
11 comparing to the geometry of the previous two bearings. Its main feature is the use of
12 “elastic hinges” in order to make the bearing more flexible. As in the case of two previous
13 bearing, the radial clearance was 20 μm . However, the bearing was made of alloyed steel. The
14 choice of steel was dictated by the need to find out if, despite a less favourable energy
15 absorption coefficient comparing to aluminium, it is acceptable material for an acoustic
16 bearing. Besides, some manufacturing reasons, such as ability to machine the bearing to
17 prescribed dimensional accuracy, also played a role in the choice of the material.
18
19
20
21
22
23
24
25
26
27
28
29
30

31 32 33 2.2 Apparatus

34 Figure 4 shows apparatus used for experimental testing. A characteristic feature of the
35 apparatus is the shaft vertically positioned and supported by an aerostatic thrust bearing
36 placed on the base plate. This apparatus was specifically designed to experimentally measure
37 the load capacity of the bearing and its dynamic stability when it operates at speed with and
38 without squeeze film ultrasonic levitation. The shaft was made of stainless steel and its
39 nominal diameter was 30 mm. It was fitted into the bearing with the radial nominal clearance
40 of 20 μm . An aerostatic thrust bearing supporting the shaft was supplied with compressed air
41 produced by an external source. Running of the shaft at speed was due to an air turbine. The
42 air turbine comprised buckets machined at both ends of the shaft to and ensure uniform
43 distribution of mass along the shaft. Three air nozzles secured to the housing of the apparatus
44
45
46
47
48
49
50
51
52
53
54
55
56
57
58
59
60
61
62
63
64
65

1 were supplying air jets tangent to the shaft's circumference. Operation of PZTs and hence the
2 deformation of the bearing tested was controlled by an amplifier and frequency generator. A
3 schematic diagram showing components of the control system is presented in Figure 5.
4

5
6
7 Position of the shaft within the journal bearing was monitored in two mutually perpendicular
8
9 planes by contactless sensors. The proximity transducer system, 3300 NSv 5 mm, for radial
10 position measurements, supplied by Bentley Nevada, was used. Before being mounted in the
11 test apparatus both sensors were calibrated using precision X-Y stage with micrometre
12 accuracy. A plot of the distance from the target surface versus the DC voltage was produced
13 and inputted into the data acquisition system employed to record shaft's movements during
14 bearing operation. The signal from the sensors located in mutually perpendicular planes was
15 recorded in real time by the data acquisition system as X and Y displacement in micro-metres.
16
17 The file was then transferred to Excel and edited. Next the X-Y graph (scatter) available in
18 Excel was used to plot experimental points for a given load on the bearing, its rotational
19 speed, and the status of PZTs (switch-on or switched-off). This was done for specified time
20 lapse of the experiment.
21
22
23
24
25
26
27
28
29
30
31
32
33
34
35
36
37
38
39

40 The apparatus was clamped to the base plate and could be tilted by desired angle Θ creating,
41 in consequence, a loading on the bearing in a controlled way. The load on the bearing (F) was
42 calculated from the expression,
43
44
45

$$46 \quad F = mgsin\Theta$$

47
48
49 Where m is the mass of the shaft, g is gravitational acceleration, and Θ is the angle of tilt.
50

51 During experimental testing three different loads on the bearing were used namely: 0.1 N
52
53 (corresponding to $\Theta = 1$ deg), 0.31 N ($\Theta = 3$ deg) and 0.62 N ($\Theta = 6$ deg).
54
55
56
57
58
59
60
61
62
63
64
65

1 Central objective of experimental testing was to determine the effectiveness of the squeeze
2 film ultrasonic levitation in mitigating the magnitude of the shaft's motion within the bearing
3 when it was running at speed and under a load.
4
5
6
7
8
9

10 2.3 Procedure

11 Testing procedure involved the following activities. Setting offset voltage, V_{off} , for PZTs which
12 produced constant initial elastic deformation of the bearing. Cyclic elastic deformation of the
13 bearing (amplitude) was controlled by the running voltage V_{amp} . Usually V_{off} was set to 70 V
14 and V_{amp} to 60 V for bearings with geometries G1 and G2. For the bearing with geometry G3
15 V_{off} was equal to 50 V and V_{amp} equal to 40 V.
16
17
18
19
20
21
22
23
24

25 A typical test involved the following.

26
27 (i) Ensuring that the shaft was in a true vertical position and floated freely on air cushion
28 created by the aerostatic bearing fitted into the base of testing apparatus.
29
30

31 (ii) Setting the offset voltage, V_{off} , to a required value so that the bearing deformed
32 accordingly.
33

34 (iii) Setting the running voltage, V_{amp} , corresponding to the amplitude of cyclic elastic
35 deformations of 40 V.
36
37

38 (iv) Operating PZTs at frequency corresponding to resonant frequency of the bearing with a
39 given geometry.
40
41
42

43 (v) Initiating rotation of the shaft at speed when it was in a vertical position (no load on the
44 bearing).
45
46
47

48 (vi) Tilting the apparatus by required angle Θ in order to exert a load on the bearing. Three
49 different loads on the bearing were used: very light load (0.1 N), intermediate load (0.31 N)
50 and substantial load (0.62 N).
51
52
53
54
55
56
57
58
59
60
61
62
63
64
65

1 First run was with switched-off PZTs. This enabled to measure the movement of the shaft
2 within the bearing with the help of two non-contact probes located at two mutually
3 perpendicular directions. Using computerised data acquisition system, continuous recording
4 of the shaft movement at every 0.1 second took place. These data allowed construction of
5 diagrams illustrating movement of the shaft's centre within the bearing operating at specified
6 speed and load. The magnitude of the shaft motion in X and Y directions provided information
7 whether operation of the bearing was stable or not. Using the same procedure, the influence
8 of PZTs switched-on on the movement of the shaft was ascertained.
9
10
11
12
13
14
15
16
17
18
19
20
21
22

23 3. Results and their discussion

24 Before experimental results are presented and discussed it is beneficial to consider potential
25 role of PZTs operation as an agent stabilising the running of a lightly loaded aerodynamic
26 journal bearing. Bearing operating without PZT switched-on behaves as a classic aerodynamic
27 bearing depending on the pressure generated in the clearance space by a well-known
28 aerodynamic mechanism. In order to achieve complete separation between the bearing and
29 the shaft a converging gap in the direction of shaft's motion is required and the process can
30 be mathematically described by the Reynolds equation modified for a compressible flow.
31 Converging gap necessitates a load on the bearing and complete separation is only attained at
32 a certain rotational velocity. With PZTs switched-on the bearing operation is affected in two
33 ways, that is through squeeze-film effect producing an extra pressure at the bearing/ shaft
34 interface and, additionally, due to preliminary static deformation of the bearing (applied
35 offset voltage) creating a geometry facilitating generation of an aerodynamic pressure even
36 with no loads on the bearing. Since three PZTs are used to elastically deform bearing's bore a
37 three-lobe geometry is easily created. This geometry significantly helps to generate
38
39
40
41
42
43
44
45
46
47
48
49
50
51
52
53
54
55
56
57
58
59
60
61
62
63
64
65

1 aerodynamic pressure (three converging gaps in the direction of shaft's motion). Additionally,
2 this characteristic geometry at the interface is fluctuating with the frequency and amplitude
3 determined by the control system of PZTs giving rise to the squeeze film pressure. Variation
4 of the squeeze film pressure around the circumference of the clearance is prescribed by the
5 geometry of elastic deformation of the bore. In the case presented in this paper, the squeeze
6 film pressure is distributed in a form of three "half-moons", spaced by 120° , and ensuring
7 stability of the shaft's motion together with its complete separation from the bearing even
8 though the shaft is stationary [23]. Thus, operation of an acoustic bearing can be depicted as
9 a cooperation of the squeeze film pressure and, after a certain rotational velocity is attained,
10 aerodynamic pressure. A mathematical model for this cooperation is being prepared and will
11 be published in due time.

12 Experimental results presented and discussed below unequivocally demonstrate beneficial
13 influence of switched-on PZTs on the operation of the bearing. The format of all figures is the
14 same, namely each one presents displacement of the shaft in X and Y directions when PZTs
15 are switched on (series 1 results) and switched off (series 2 results). The effectiveness of PZTs
16 action is measured by the ratio (called R1 coefficient) of maximum displacement in X direction
17 recorded for the bearing with PZTs switched on to the maximum displacement in X direction
18 recorded for the bearing with PZTs switched off. Coefficient called R2 is the ratio of maximum
19 displacements in Y direction observed for the bearing with PZTs switched on to that when
20 PZTs were switched off. Although it is not the perfect way to quantify the influence of PZTs on
21 the bearing's dynamic performance, nevertheless, if used in a consistent way it provides a
22 convenient means to assess the usefulness of applying PZTs technology to a lightly loaded,
23 high speed aerodynamic journal bearing. Three different loads were used, namely 0.1 N,
24 0.31 N, and 0.62 N. Consequently, extreme movements of the shaft were observed at

different rotational speeds, depending on the load applied and geometry of the bearing.

Details for each bearing tested are provided below.

3.1 G1 bearing

Dynamic performance of G1 bearing (see Figure 1) at three different loads is shown in Figures 6-8. Figure 6 illustrates performance of the bearing with geometry 1 running at speed of 6450 rpm and PZTs frequency of 78.8 kHz under the load 0.1 N. This frequency of PZTs operation corresponds to a resonance frequency of the bearing with geometry estimated through a modal analysis. It can be observed that the benefit of switching on PZTs, as measured by the magnitude of R1 and R2 coefficients, is undisputable. When the PZTs were switched off, the bearing running at very light load exhibited large displacements of the shaft in both directions almost reaching radial clearance. Switching on PZTs reduced the shaft motion by approximately 35 percent ($R1 = 0.634$ and $R2 = 0.641$). However, when the load on the bearing was increased to 0.31 N, dynamic performance of the bearing (as measured by the magnitude of shaft's motion in X and Y directions) changed and largest shaft's displacements were observed at 10560 rpm (see Figure 7). But, switching on PZTs reduced the shaft motion but by a significantly reduced amount, comparing to the previous case. Coefficient R1 and R2 are 0.862 and 0.679 respectively. This can be explained by the fact that as the load on the bearing increased, the bearing became more stable which is a well-known fact for aerodynamic journal bearings. This is confirmed by the results shown in Figure 8. Increasing the load on the bearing to 0.62 N resulted, basically, in the same dynamic performance as that observed for the load of 0.31 N. Quantitatively, this observation is confirmed by the magnitudes of R1 and R2 coefficients. They are both quite similar to those of the previous load case. Again, switching on PZTs helped to reduce the shaft's motion but not as much as in

1 the case of a very light load on the bearing that is 0.1 N. Again, it looks like that the bearing
2 running under increased load is having enhanced inherent stability and the use of PZTs is not
3 necessarily required.
4
5
6
7
8
9

10 3.2 G2 bearing

11
12 Figures 9-11 illustrate dynamic performance of the bearing with geometry 2 (G2). For this
13 geometry PZTs were operating with frequency of 36.7 kHz and this reflects the fact of a more
14 flexible geometry used. Figure 9 concerns movements of the shaft when the load on the
15 bearing was 0.1 N and rotational speed equal to 12817 rpm. Figure 10 represents data
16 recorded for the bearing with the same rotational speed but with load of 0.31 N. Finally,
17
18 Figure 11 provides data for the bearing running at the load of 0.62 N.
19
20
21
22
23
24
25
26

27 Using coefficients R1 and R2 it is permissible to say that again the largest effect of PZTs being
28 switched on is for the lightest load. For this load $R1 = 0.610$ and $R2 = 0.530$ which is
29 approximately equivalent to 40 per cent reduction of shaft's motion within the bearing. This is
30 quite remarkable stabilisation effect provided by PZTs.
31
32
33
34
35
36
37

38 When the load was increased to 0.31 N the effect of PZTs switched on is smaller as $R1 = 0.716$
39 and $R2 = 0.677$ giving equivalent of about 30 per cent reduction in shaft's motion. This is in
40 line with what was found for bearing G1.
41
42
43
44

45 The highest loaded bearing (0.62 N) behaved quite similarly to that loaded by 0.31 N. This is
46 shown in Figure 11. With $R1 = 0.707$ and $R2 = 0.660$ the reduction in shaft's motion is not
47 much different to that observed for the bearing running under the load of 0.31.
48
49
50
51
52
53

54 The rationale for this dynamic performance is as that advanced before – loaded aerodynamic
55 bearing acquires inherent stability hence the effect of PZTs operation is not as significant as
56 for a lightly loaded bearing (0.1 N).
57
58
59
60
61
62
63
64
65

3.3 G3 bearing

As mentioned earlier bearing G3 had rather elaborate geometry and was much more flexible than the previously discussed two bearings. Therefore, its resonance frequency was equal to 8.8 kHz and that was the frequency at which PZTs operated when testing was carried out. At all three loads the bearings run at 13275 rpm.

Figure 12 data were obtained at the lightest load used during testing that is 0.1 N. As in the case of previous two bearings the stabilising effect of PZTs is greatest. Coefficients R1 and R2 are equal to 0.432 and 0.487 respectively which corresponds to over 50 per cent reduction in shaft's motion. This is quite significant effect. Figure 13 contains data for the operation of the bearing G3 at the load of 0.31 N. Reduction in shaft's motion is much less ($R1 = 0.816$ and $R2 = 0.717$) and that is in line with the results reported earlier. Clearly, more loaded aerodynamic journal bearing usually demonstrates increased inherent stability of motion. Similarly, results shown in Figure 14 (load on the bearing 0.62 N) confirm the trend of reduced effectiveness of PZTs due to increased inherent stability of higher loaded bearings. This is confirmed by $R1 = 0.738$ and $R2 = 0.660$ which are slightly lower than at the load of 0.31 N. Apparently, the effect of preliminary static deformation of the bearing mentioned above played here much more significant role. The bearing was relatively flexible and it was quite easy to deform its initial circular bore to a three lobe configuration which is known to secure stable operation of an aerodynamic journal bearing.

3.4 Comparison of performance

Taking into account results of experimental testing the dynamic performance of three bearings with different geometries can be ranked as follows: (i) G3 bearing, (ii) G2 bearing,

1 and (iii) G1 bearing. Incidentally, this ranking is similar to that presented and discussed in the
2 earlier paper dealing with the start-stop performance of these three bearings [23]. The
3 current ranking is based on the magnitude of shaft's motion within the very lightly load
4 bearing as expressed quantitatively by coefficients R1 and R2. The justification for the ranking
5 could be argued as follows. Out of the three geometries, the one denoted G3 (see Figure 3)
6 equips the bearing with the highest flexibility due to so called "elastic hinges". Therefore, the
7 bearing can be elastically deformed into the three lobe configuration with ease facilitating
8 strong squeeze-film effect. Also, the presence of elastic hinges significantly reduces the force
9 generated by PZTs and required to generate desired magnitude of elastic deformation. This is
10 quite apparent in view of the other two geometries used. Both of them make the bearing
11 much stiffer, hence the magnitude of elastic deformation is much less than that achievable
12 for G3.
13
14
15
16
17
18
19
20
21
22
23
24
25
26
27
28
29

30 However, from the practical and manufacturing point of view, G3 is a complicated structure
31 comparing to G1 and G2. Thus, the apparent advantages of G3 are not so obvious when one
32 considers practicalities.
33
34
35
36
37
38
39
40

41 4. Conclusions

42 Based on the results presented in this paper the following conclusions can be formulated.

- 43 1. Results clearly demonstrate that the squeeze-film acoustic levitation substantially mitigates
44 the magnitude of shaft's motion within the bearing.
45
- 46 2. An important factor in the dynamic performance of the bearing is its geometry.
47
- 48 3. Geometry equipping the bearing with a low overall stiffness secures better dynamic
49 performance in terms of reduced shaft's motion as expressed by coefficients R1 and R2.
50
51
52
53
54
55
56
57
58
59
60
61
62
63
64
65

1
2
3
4
5
6
7
8
9
10
11
12
13
14
15
16
17
18
19
20
21
22
23
24
25
26
27
28
29
30
31
32
33
34
35
36
37
38
39
40
41
42
43
44
45
46
47
48
49
50
51
52
53
54
55
56
57
58
59
60
61
62
63
64
65

4. Bearing with higher flexibility is able to produce larger elastic deformation amplitude securing enhanced ability to separate interacting surfaces.

5. Acknowledgement

The authors would like to acknowledge the financial support for the research reported in this paper by the grant from the National Centre of Science, Poland (grant no.: 2012/07/B/ST8/03683).

6. References

1. Vandaele, V., Lambert, P., Delchambre, A., Non-contact handling in microassembly: Acoustical levitation, *Precision Engineering*, 29, 491-505, 2005.
2. Poynting, J.H. and Thomson, J.J., A textbook of Physics, Charles Griffin & Co., 1904.
3. King, L.V., On the acoustic radiation pressure on spheres, *Proc. R. Soc., London*, 1934.
4. Hasegawa, T., Acoustic radiation forces on a solid elastic sphere, *Acoustical Society of America*, 46, 1139, 1969.
5. T.F.W. Embleton, Mean force on a sphere in a spherical sound field, pt. I (theoretical), *J. Acoust. Society of America*, 26, 40, 1954.
6. Westervelt, P.J., The mean pressure and velocity in a plane acoustic wave in a gas, *J. Acoust. Society of America*, 22, 319-327, 1950.
7. Westervelt, P.J., The theory of steady forces caused by sound waves, *J. Acoust. Society of America*, 23, 312-315, 1951.
8. Westervelt, P.J., Acoustic radiation pressure, *J. Acoust. Society of America*, 29, 26-29, 1957.
9. Salbu, E.O.J., Compressible squeeze-films and squeeze bearings, *J. Basic Eng.*, 86, 355-

366, 1964.

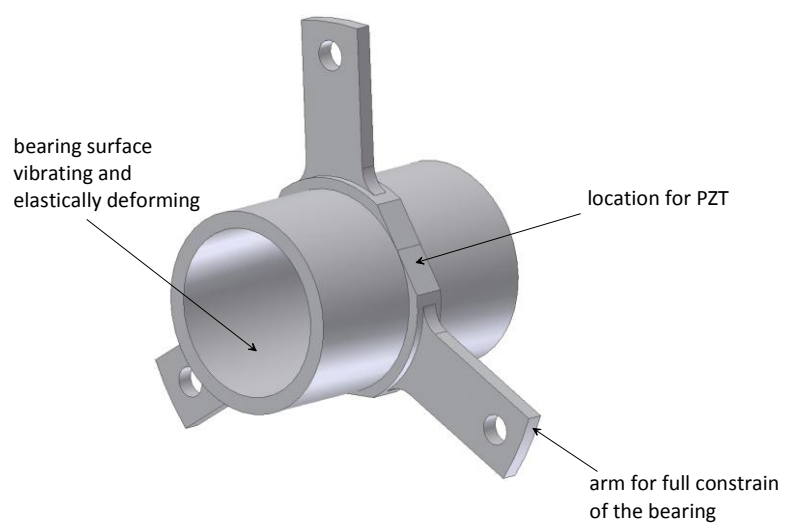
10. Warnock, L.F., Dynamic gas film supported inertial instrument, US Patent No. 3339421, 1967.
11. Farron, T.B.R., Squeeze-film bearings, US Patent No. 3471205, 1969.
12. Scranton, R.A., Planar and cylindrical oscillating pneumatodynamic bearings, US Patent No. 4666315, 1987.
13. Zhao, S., Wallaschek, J., Design and modeling of a novel squeeze-film journal bearing, Proc. 2009 IEEE Int Conf Mechatronics and Automation, Changchun, China, Aug 9-12, 2009.
14. Stolarski, T.A. and Wei Chai, Self-levitating air contacts, Int. J. Mech. Sci., 48, 601-620, 2006.
15. Stolarski, T.A. and Wei Chai, Load-carrying capacity generation in squeeze-film action, Int. J. Mech. Sci., 48, 736-741, 2006.
16. Stolarski, T.A. and Wei Chai, Inertia effect in squeeze-film air contact, Tribology International, 41, 716-723, 2008.
17. Stolarski, T.A., Performance of a self-lifting linear air contact, Proc. IMechE, part C, J. Mechanical Engineering Science, 221, 1103-1115, 2007.
18. Stolarski, T.A., Self-lifting contacts – From Physical Fundamentals to Practical Applications, Proc. IMechE, part C: J. Mech. Eng. Sci., 220, 1211-1218, 2006.
19. Ha, D.N. Stolarski, T.A., Yoshimoto, S., An aerodynamic bearing with adjustable geometry and self-lifting capacity, Proc. IMechE, part J, J. Engineering Tribology, 219, 33-39, 2005.
20. Ha, D.N. Stolarski, T.A., Yoshimoto, S., An aerodynamic bearing with adjustable geometry and self-lifting capacity, Proc. IMechE, part J, J. Engineering Tribology, 219, 33-39, 2005.
21. Xue, Y., Stolarski, T.A., Yoshimoto, S., Air journal bearing utilizing near field acoustic

levitation - stationary shaft case, Proc. IMechE, part J, J. Engineering Tribology, 225, 120-127, 2011.

22. Stolarski, T.A., Running characteristics of aerodynamic bearing with self-lifting capability at low rotational speed, Advances in Tribology, 2011.

23. Stolarski, T.A., Gawarkiewicz, R., Tesch, K., Acoustic journal bearing – A search for adequate configuration, Tribology International, 92, 387-394, 2015.

1
2
3
4
5
6
7
8
9
10
11
12
13
14
15
16
17
18
19
20
21
22
23
24
25
26
27
28
29
30
31
32
33
34
35
36
37
38
39
40
41
42
43
44
45
46
47
48
49
50
51
52
53
54
55
56
57
58
59
60
61
62
63
64
65

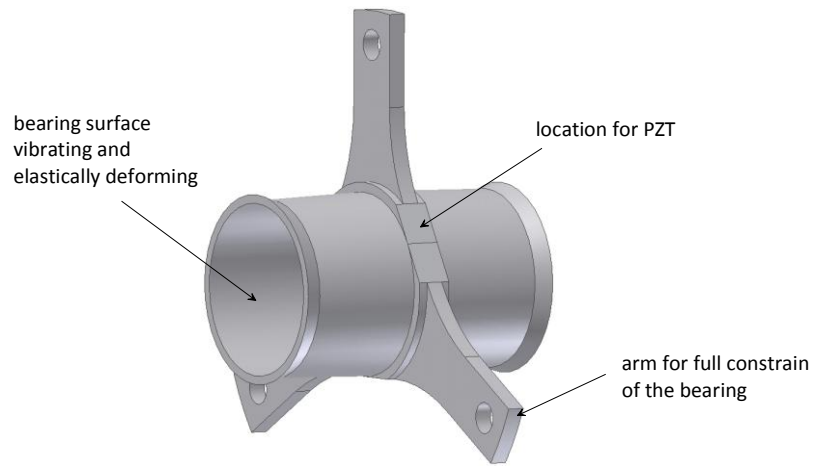


(a)

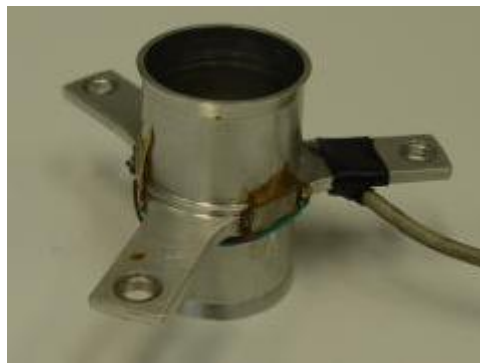


(b)

Figure 1

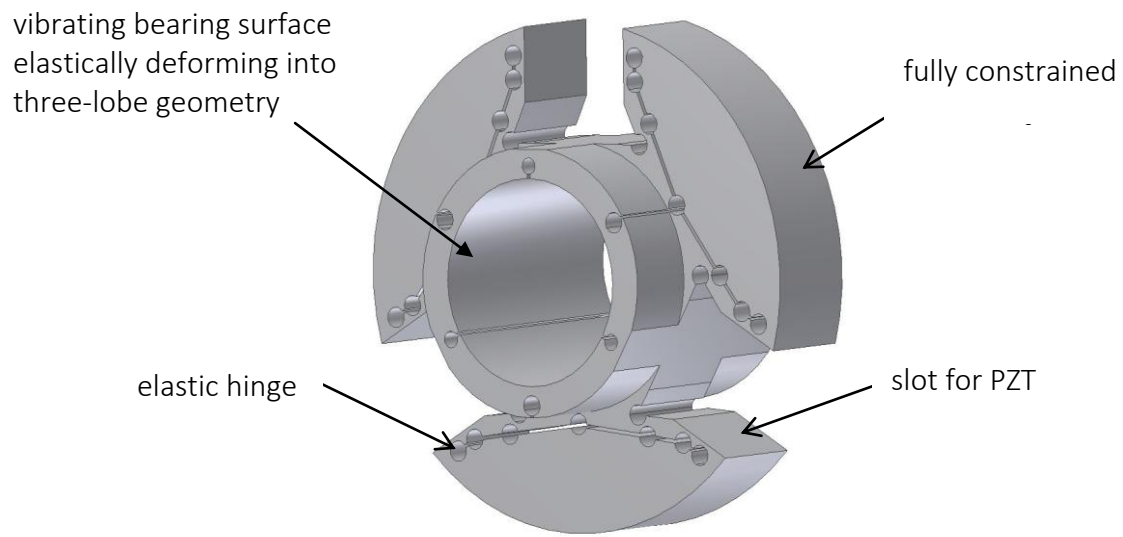


(a)

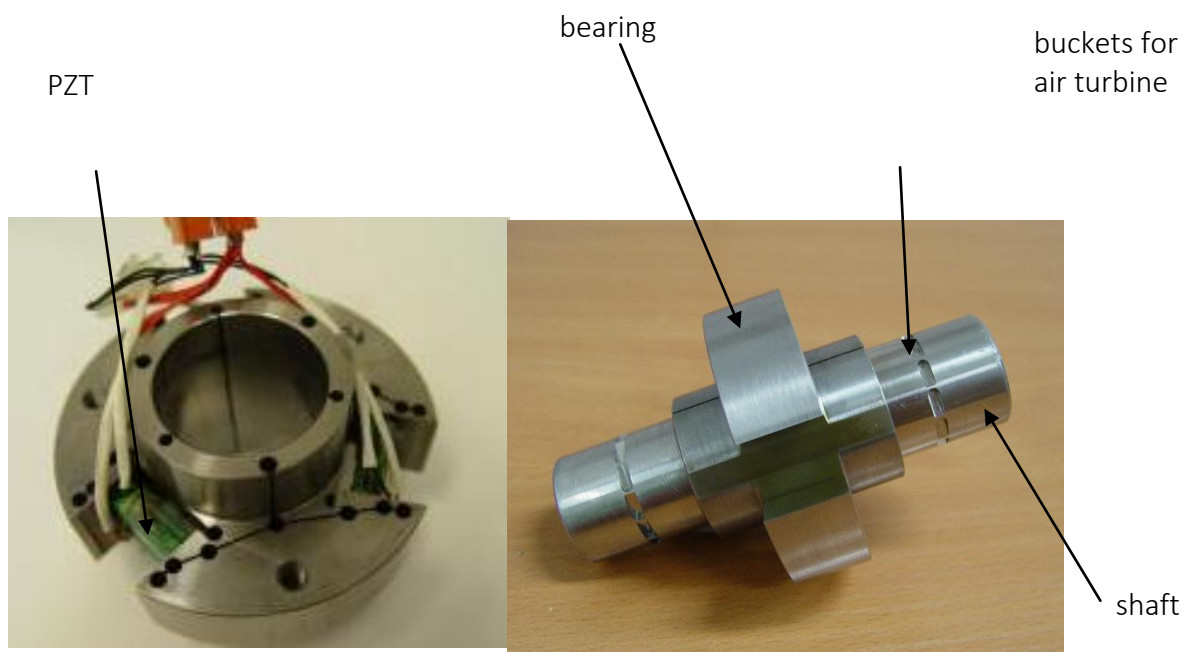


(b)

Figure 2



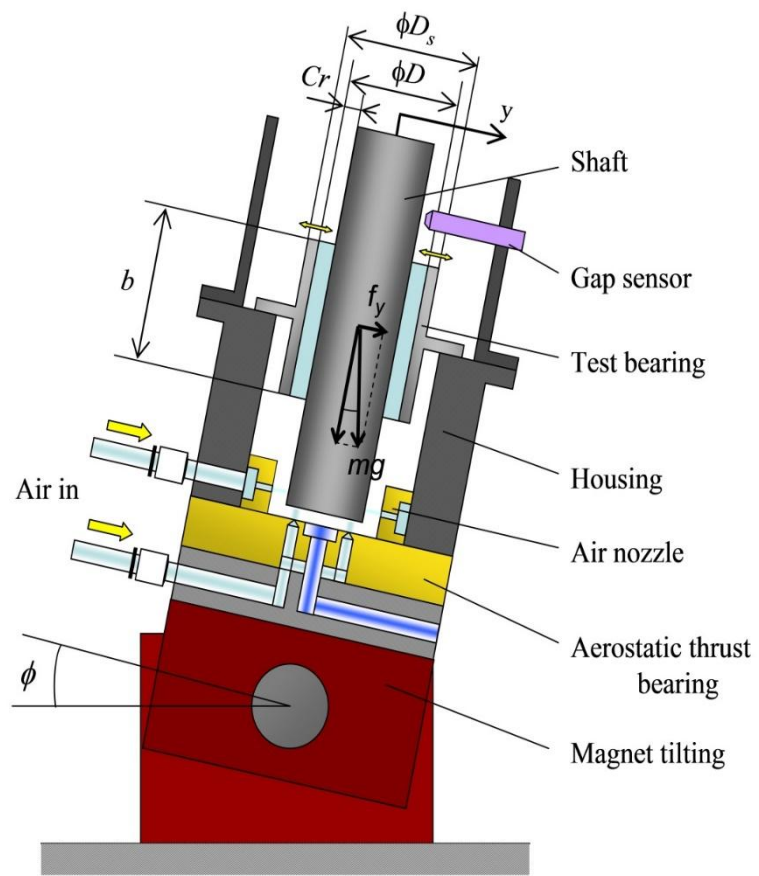
(a)



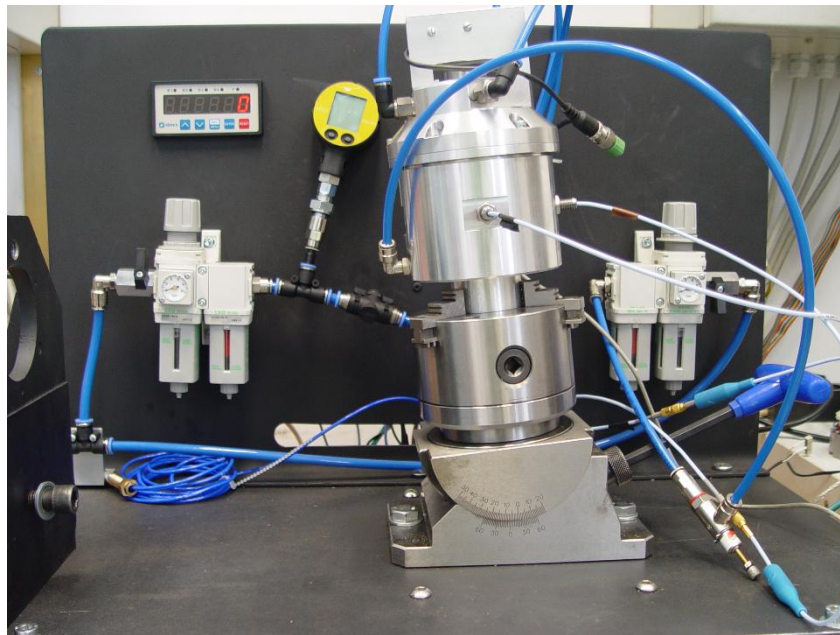
(b)

(c)

Figure 3



(a)



(b)

Figure 4

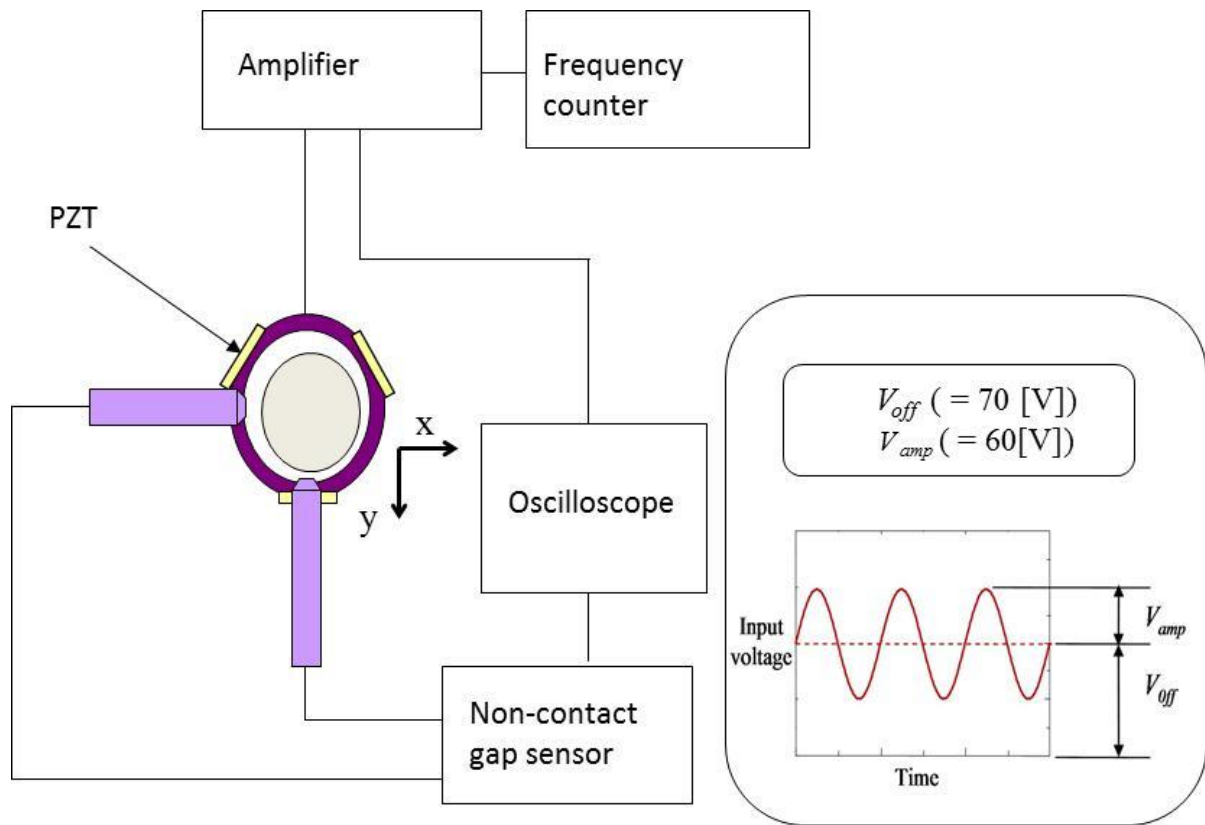


Figure 5

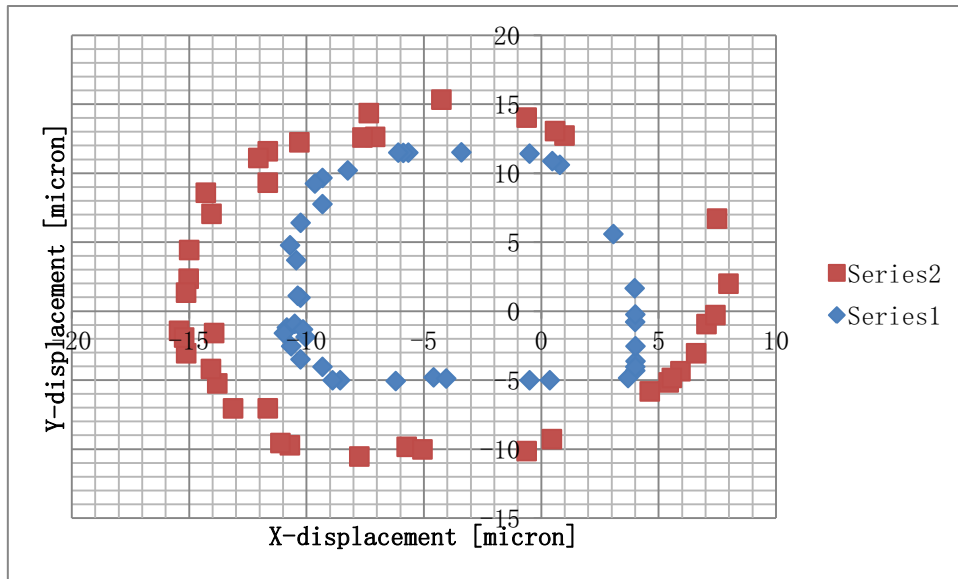


Figure 6

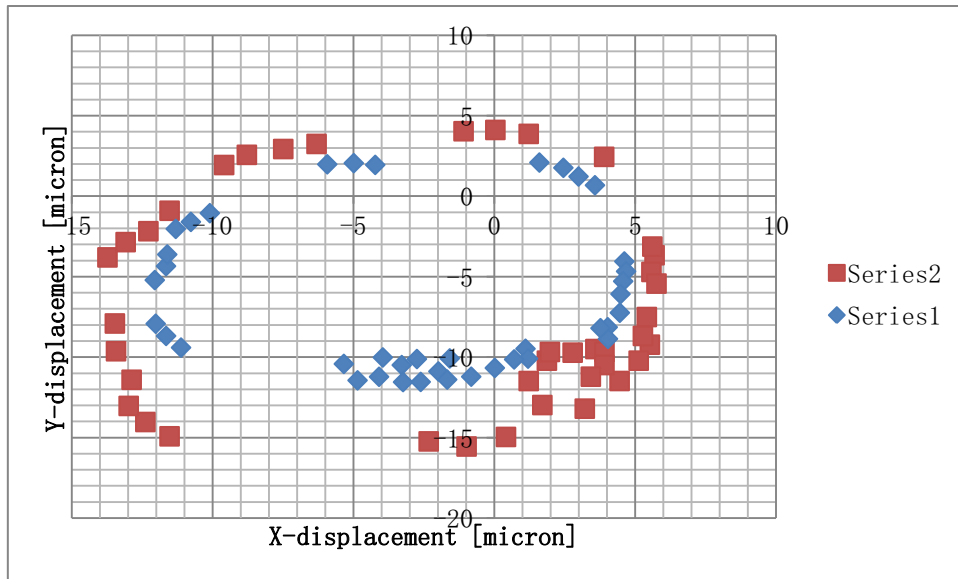


Figure 8

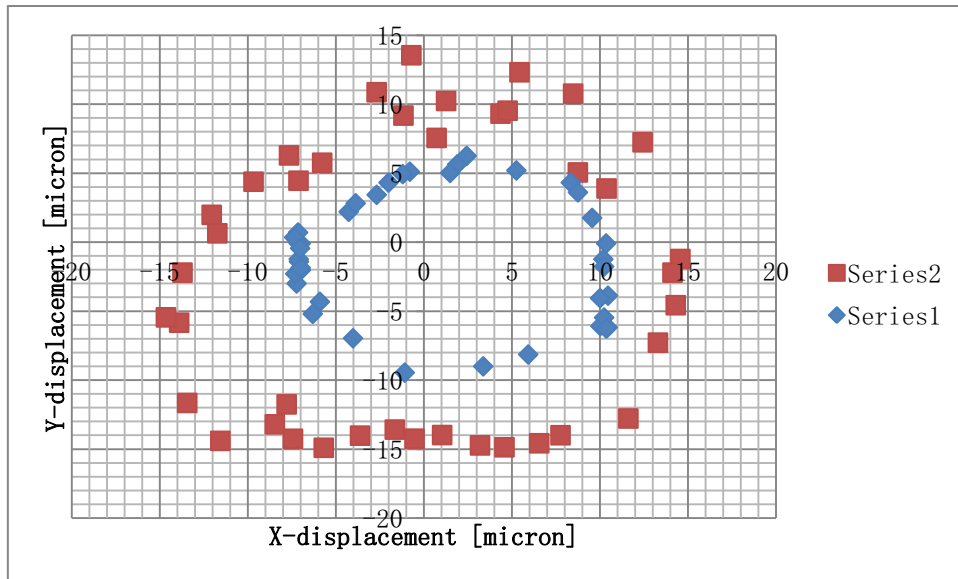


Figure 9

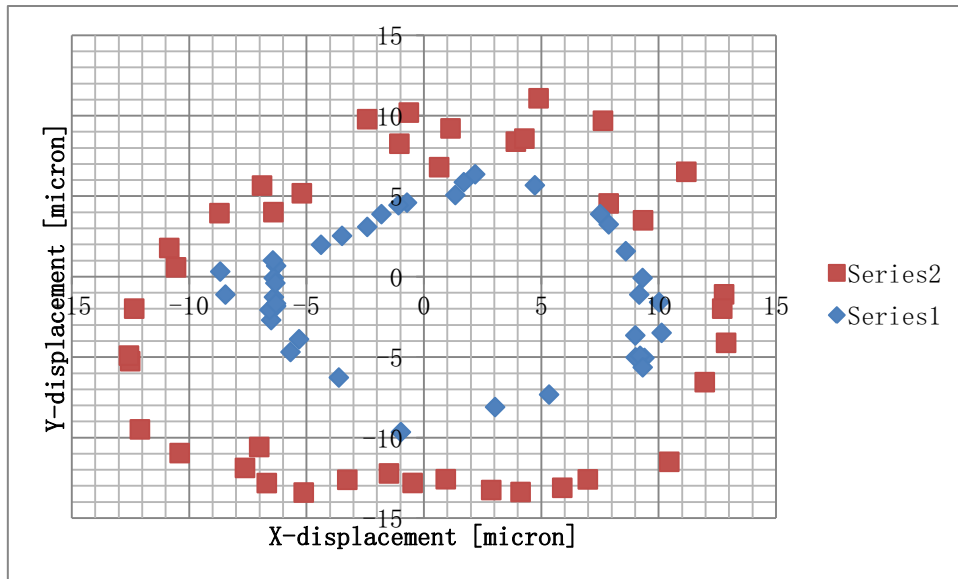


Figure 10

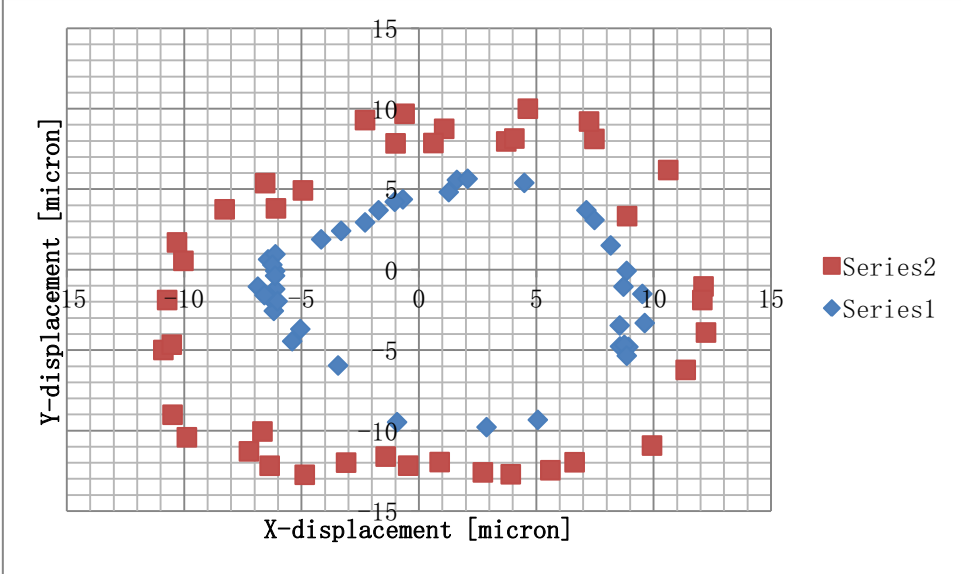


Figure 11

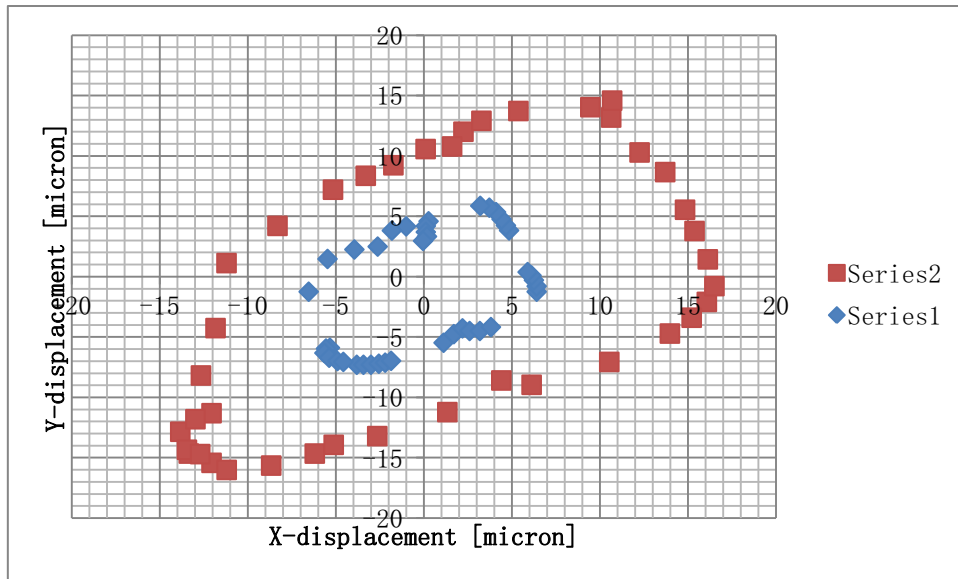


Figure 12

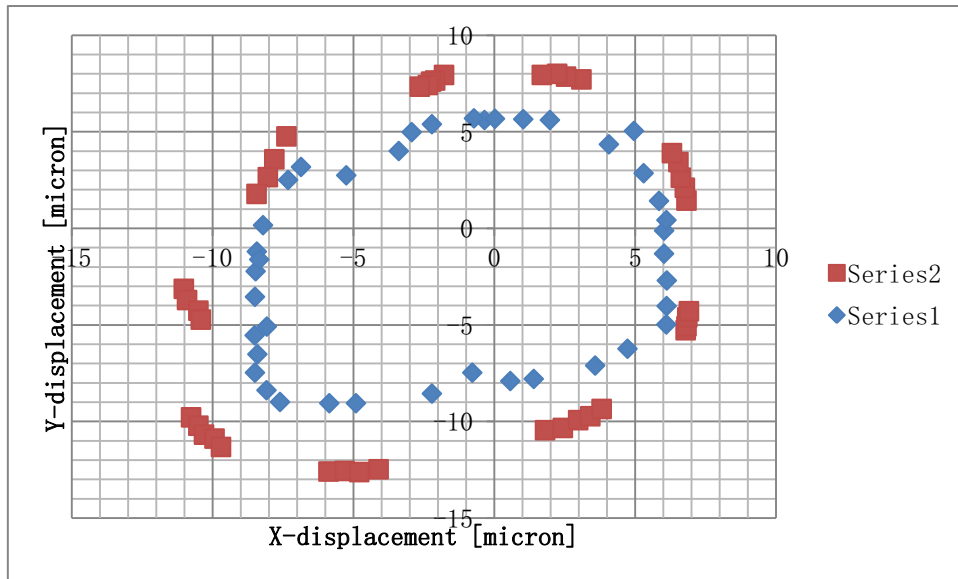


Figure 13

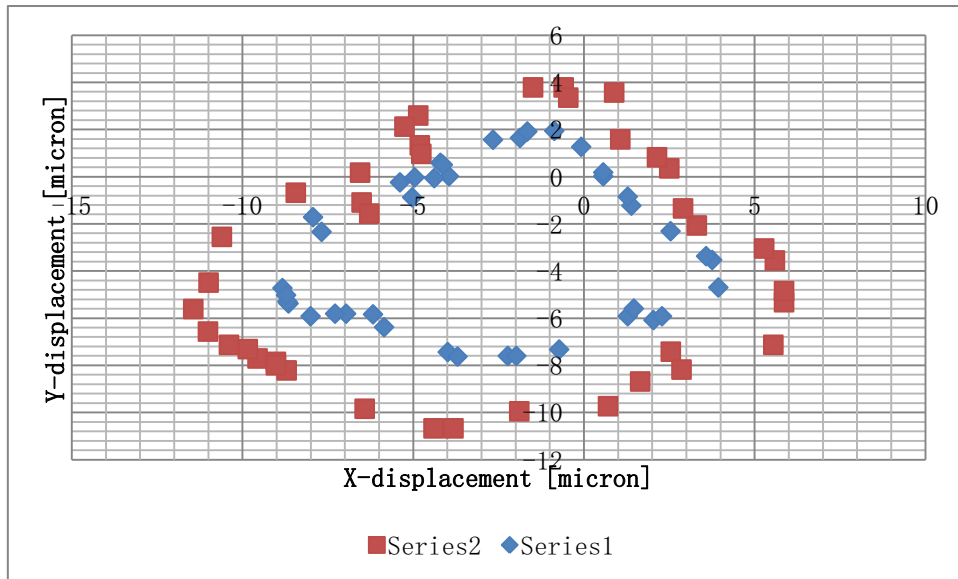


Figure 14